Induction of relaxor state in ordinary ferroelectrics by isovalent ion substitution: A pretransitional martensitic texture case

M. H. Lente,* E. N. Moreira, D. Garcia, and J. A. Eiras
Departamento de Física-Grupo de Cerâmicas Ferroelétricas, Universidade Federal de São Carlos, São Carlos SP, CEP 13560-905 Brazil

P. P. Neves, A. C. Doriguetto, V. R. Mastelaro, and Y. P. Mascarenhas
Instituto de Física de São Carlos, Grupo de Crescimento de Cristais e Cerâmicas, Universidade de São Paulo, São Carlos SP, CEP 13566-590 Brazil

(Received 10 October 2005; published 17 February 2006)

The understanding of the structural origin of relaxor ferroelectrics has been doubtlessly a long-standing puzzle in the field of ferroelectricity. Thus, motivated by the interest in improving the comprehension of this important issue, it a framework is proposed for explaining the origin of the relaxor state in ordinary ferroelectrics induced via the isovalent-ion substitution. Based on the martensitic transformation concepts, it is proposed that the continuous addition of isovalent ions in a so-called normal ferroelectric decreases considerably the elastic strain energy. This results in a gradual transformation of ferroelectric domain patterns from a micrometer polydomain structure (twins), through single domains, to nanometer-polar-"tweed" structures with glasslike behavior, that are, in turn, strongly driven by point defects and surface effects. The electrical interaction between these weakly coupled polar-tweed structures leads to a wide spectrum of relaxation times, thus resulting in a dielectric relaxation process, the signature of relaxor ferroelectrics.

DOI: 10.1103/PhysRevB.73.054106 PACS number(s): 77.22.Ch, 77.22.Gm, 77.84.Dy

I. INTRODUCTION

The investigation of the physical origin of relaxor ferroelectrics (relaxors) is doubtlessly one of the most challenging tasks of the field of ferroelectricity. In contrast to ordinary ferroelectrics (also so-called "normal" ferroelectrics), relaxors have the following remarkable features:[1–6] (i) an existence of local lattice disorder, (ii) no necessarily, macroscopic structural phase transition; (iii) the absence of macroscopic spontaneous polarization, (iv) the maximum of dielectric constant shifts toward higher temperatures with increasing frequency (dielectric relaxation), and (v) the presence of nanometric-polar regions immerse in a highly polarizable host lattice. With regard to the influence of the dynamics of such nanometric-polar regions on the dielectric properties, various phenomenological models have been proposed in the literature. The superparaelectric,[7] dipolar glass,[8] quenched random-field,[9] and spherical random-bond-random-field models[10] are certainly the most known. However, the nature of the relaxor behavior cannot be completely understood based only on the kinetics. Thus, insights into the key structural origin of relaxors are still needed.

From the structural point of view, massive investigations have been focused on $A(B'B'')O_3$ complex perovskites. A typical example is $Pb(Mg_{1/3}Nb_{2/3})O_3$ (PMN), which is considered the prototype material for a fundamental understanding of relaxor ferroelectrics.[11,12] The investigation of such a relaxor system has been centered on the determination of how chemical, compositional, and/or orientational disorders influence the formation of polar nanoregions.[5,12,13] Furthermore, starting from the relaxor state, it is observed that ferroelectric long-range order and structural phase transitions can be gradually induced in the PMN by the substitution of Mg^{2+}/Nb^{5+} for Ti^{4+}.[14–16]

On the other hand, ordinary ferroelectric materials are hybrid ferroics that are characterized by a strong ferroelastic-ferroelectric coupling.[17–20] The remarkable feature of ordinary ferroelectrics is the formation of well-defined domain and domain wall structures (twins) when they are cooled from the paraelectric to the ferroelectric phase to minimize the elastic strain energy.[21–24] From the point of view of elastic effects, the situation of ferroelectric twins is analogous to twins in ferroelastic materials, which is caused by martensitic transformation.[25,26] Rather, the paraelectric-ferroelectric phase transition is usually followed by a displacive structural transition[27,28] accompanied by a relative large lattice strain, whose elastic long-range interactions play a major role in determining both domain morphology and domain growth law in ferroelectric perovskites.[20,29,30]

Of particular interest is the prototypical ordinary ferroelectric lead titanate, $PbTiO_3$, and the closely related system lead zirconate-titanate, $Pb(Zr,Ti)O_3$, which exhibit long-range ferroelectric order, micrometer domain and/or domain wall structures and do not show any frequency dispersion (relaxational effect) in the audio frequency range. Nevertheless, it is well known that some chemical substitutions, such as La^{3+} at the Pb^{2+} site to form $(Pb,La)(Zr,Ti)O_3$ ceramics, induce a peculiar diffuse phase transition with frequency dispersion.[31] It is widely believed that both La^{3+} aliovalent ions and/or oxygen vacancies (necessary to preserve charge neutrality) break the translational symmetry of the lattice and represent a type of disorder responsible for the formation of polar nanodomains and, consequently, the relaxor feature.[31–34] However, recent experimental results have remarkably revealed that the origin of the relaxor behavior is much beyond the conventional thoughts. Indeed, it has been shown that the relaxor properties can be induced in ordinary ferro-

electrics via isovalent-ion substitution or merely via grain-size reduction,[35–37] even in simple perovskite ferroelectrics (ABO_3) in which, in principle, no disorder is expected.[35] Therefore, a more general theory that is able to explain the normal-relaxor transition is still opened.

Motivated by the interest in expanding the comprehension of the structural origin of relaxor ferroelectrics, it is investigated in this work the nature of the crossover from the ordinary ferroelectric to the relaxor state in $(Pb_{1-x}Ba_x)(Zr_{0.65}Ti_{0.35})O_3$ ceramics through dielectric and structural characterizations. A reinterpretation of the concepts of the formation of the relaxor state, starting from an ordinary ferroelectric host lattice, is proposed in terms of the evolution of ferroelectric-ferroelastic twin patterns by successive martensitic transformations.

II. EXPERIMENTAL PROCEDURE

$(Pb_{1-x}Ba_x)(Zr_{0.65}Ti_{0.35})O_3$ ceramics with $0 \leqslant x \leqslant 0.40$, hereafter labeled from PBZT00 to PBZT40, were prepared by a conventional mixed oxide method. It must be stressed that the substitution of Pb^{2+} for Ba^{2+} is an isovalent substitution, in which no formation of point defects (vacancies) due to charge compensation is expected. The raw materials were mixed in polyethylene bottle containing zirconium cylinders and distilled water by 1.5 h in a ball mill. After drying at $\approx$373 K the powders were calcined at different temperatures for 3.5 h and then milled for 15 h.

Disks with 20 mm in diameter and 3 mm in thickness were obtained by uniaxial and isostatic pressing. Several tests, varying the time and the temperature of sintering, were realized to determine the optimized sintering conditions, which minimize the mass losses (due to PbO volatilization) and enhance the sample densities. The samples were sintered into closed Al_2O_3 crucibles, at a saturated PbO atmosphere, and the highest densified samples were chosen for the physical characterization.

The room temperature x-ray diffraction (XRD) measurements were done at the Brazilian Synchrotron Light Laboratory facility (LNLS) using the D10B-XPD beam line. The XRD patterns were collected using a Huber diffractometer with geometry θ-2θ, $\lambda = 1.529\,59$ Å. The data were collected with step size of 0.02°. The count time was 0.5 seg/step from 20 to 90° 2θ and 1.0 sec/step from 90 to 120° 2θ. Since the synchrotron beam decays with time, the measured intensity was normalized using the monitor counts. A silicon single crystal analyzer was mounted in the diffraction path between the sample and the detector in order to improve the instrumental resolution and peak-to-background discrimination. The refinement of the structure was carried out using the Rietveld method.[38] The program used in the refinements was the general structure analysis system package.[39] This procedure was described in detail previously.[40] The theoretical density D_x was calculated using these lattice parameters. The morphologic aspects of the microstructure were observed by scanning electron microscopy.

To perform dielectric characterizations, disk-shape ceramic bodies were polished and annealed at 900 K for 1 h to release mechanical stresses introduced by the polishing process. Silver electrodes were deposited onto the surfaces by sputtering. Computer assisted dielectric characterization, as a function of frequency (from 100 Hz to 1 MHz), were made employing an impedance analyzer HP 4194A at a constant cooling rate of 2 K/min.

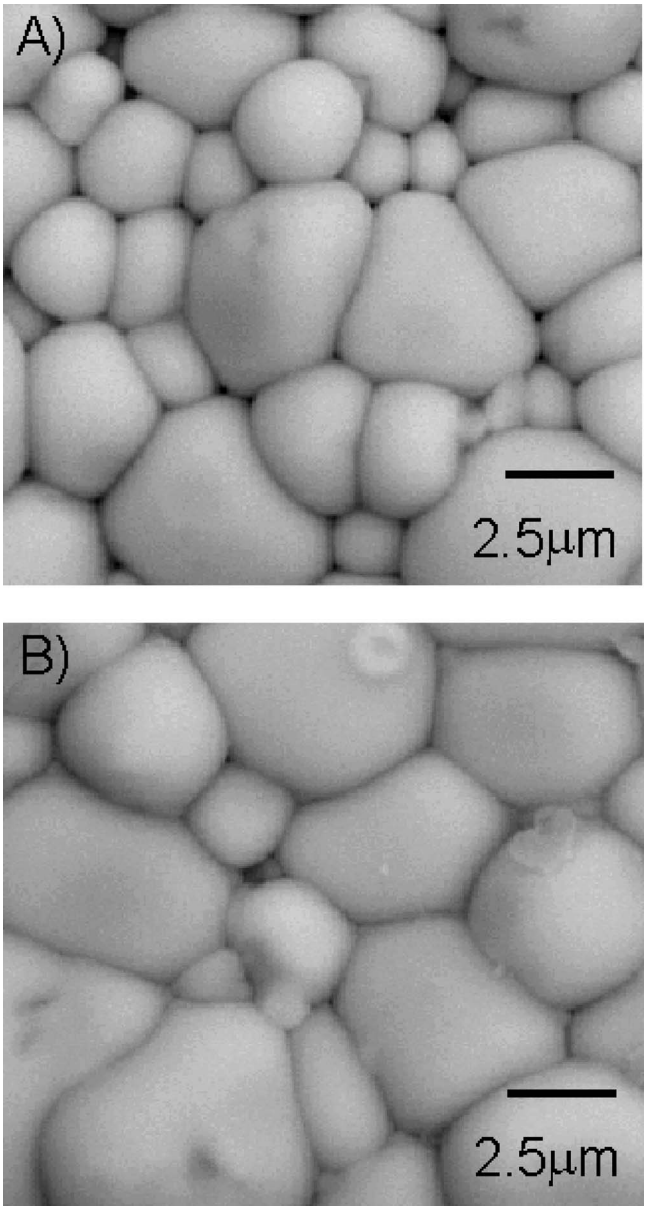

FIG. 1. Scanning electron micrographs of the sintered-sample surfaces of $(Pb_{1-x}Ba_x)(Zr_{0.65}Ti_{0.35})O_3$ samples for (a) $x=0.20$, and (b) $x=0.40$.

III. RESULTS AND DISCUSSION

Figure 1 shows the SEM for the PBZT20 and PBZT40. It is verified that the average grain size increases with increasing the Ba^{2+} content, probably due to the higher sintering temperature, although maintaining the same order of magnitude. Thus, no significant changes in the physical properties are expected due to the grain-size variation.

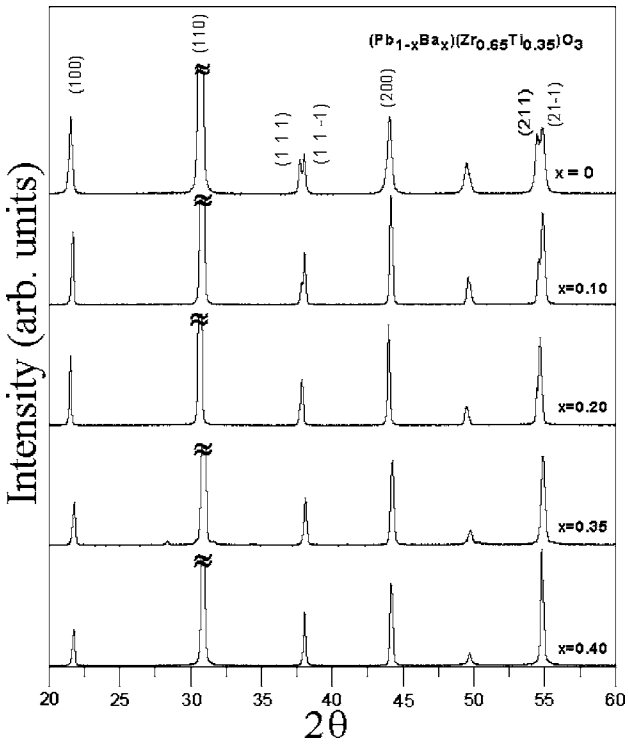

FIG. 2. X-ray diffraction patterns, at room temperature, of the PBZT compositions obtained in the optimized conditions of sintering (see Table I).

Figure 2 shows the x-ray diffraction patterns of all sintered PBZT compositions. Table I summarizes the sintering conditions and the density values (theoretical and experimental) of the sintered samples. The data reveal that all obtained samples presented high-density values ($\geqslant 96.4\%$) and only the single-perovskite phase. It is also verified that the samples with lower Ba^{2+} content present the rhombohedral symmetry ($R3c$) slightly distorted from the average cubic one, while the PBZT40 is cubic in average.

Figure 3 presents the cell parameter and the unit-cell distortion ($90°$-α_R) dependence on the Ba^{2+} content obtained from the XRD-Rietveld refinement. It is observed in Fig. 3 that the structural spontaneous strain (unit-cell distortion, $90°\,\alpha_R$) decreases with increasing the barium amount and tends clearly to vanish for the PBZT30 and PBZT40 samples. Therefore, this result reveals clearly that a spontaneous structural-like phase transition from rhombohedral to

TABLE I. Sintering conditions, structural parameters, theoretical densities, D_x, and experimental relative apparent densities for $(Pb_{1-x}Ba_x)(Zr_{0.65}Ti_{0.35})O_3$ compositions.

x	Sintering conditions	D_x (g/cm^3)	Relative density (%)
0.00	1473 K/3.5 h	7.79	96.4
0.10	1473 K/3.5 h	7.77	97.4
0.20	1523 K/3.5 h	7.56	98.7
0.35	1548 K/3.5 h	7.41	97.2
0.40	1603 K/1.0 h	7.29	96.5

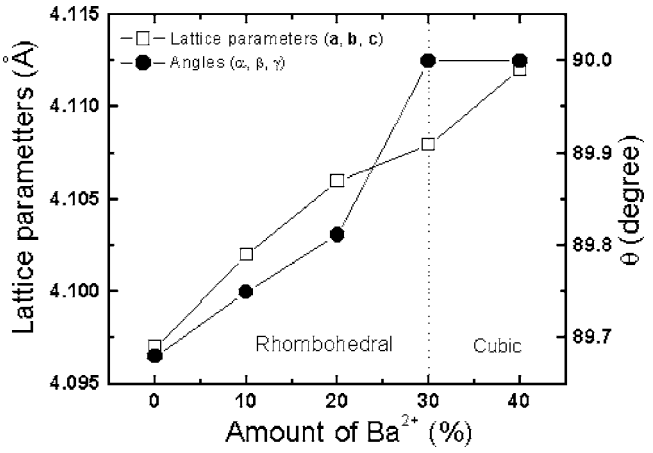

FIG. 3. (a) Cell parameter and unit cell distortion ($90°$-α_R) dependence on the Ba^{2+} content.

cubic occurs for $0.30 \leqslant x \leqslant 0.40$. This behavior has also been found in many other ferroelectric materials such as lanthanum-modified lead titanate,[31,32,40,41] although the crossover from the distorted phase (tetragonal) to a cubic one occurs for a much smaller amount of doping element.

The temperature dependence of the relative electrical permittivity (ε'), measured at 100 kHz, for all PBZT compositions is shown in Fig. 4(a). On the other hand, Fig. 4(b) depicts the temperature and frequency dependence of ε' of $(Pb_{1-x}Ba_x)(Zr_{0.65}Ti_{0.35})O_3$ for $x=0$ and $x=0.40$. The results in Fig. 4(a) reveal a remarkable reduction of the temperature of the maximum dielectric permittivity (T_m) and an increase in the diffuseness of the dielectric permittivity peak by increasing the Ba^{2+} content. Furthermore, in contrast to $x=0$, it is verified in Fig. 4(b) that for $x=0.40$ the maximum of dielectric permittivity becomes clearly frequency dependent, thus revealing the relaxor feature. Thus, in accordance with the structural results (Fig. 3), it is verified that the appearance of the normal to relaxor crossover in the dielectric measurements coincides with the induced structural-like phase transition from rhombohedral to cubic for samples containing the highest amount of barium. Similar dielectric and structural behaviors have also been obtained for lanthanum-modified lead zirconate-titanate ceramics in the La^{3+}-concentration range of $0.06 \leqslant x \leqslant 0.09$.[31,41,42]

As discussed in the Introduction, it is proposed that the disruption of the translational periodicity of the lattice via aliovalent-ion substitution is responsible for the crossover between the normal to the relaxor state.[31–34] However, it must be emphasized that the isovalent substitution of Pb^{2+} for Ba^{2+} does not create, in principle, any kind of vacancy. Therefore, the first conclusion that can be reached is that the disruption of the translational periodicity of the lattice via aliovalent-ion substitution, which reflects mainly in the formation of vacancies, is not exclusively the main cause of the normal-relaxor crossover. In addition, the antiferroelectric-ferroelectric coexistence as the origin of the relaxor behavior[43–45] is not considered here, since the $Pb(Zr_{0.65}Ti_{0.35})O_3$ composition is not in the vicinity of a morphotropic phase boundary (rhombohedral-tetragonal).[46] Thus, it is believed that the key to improve the understanding

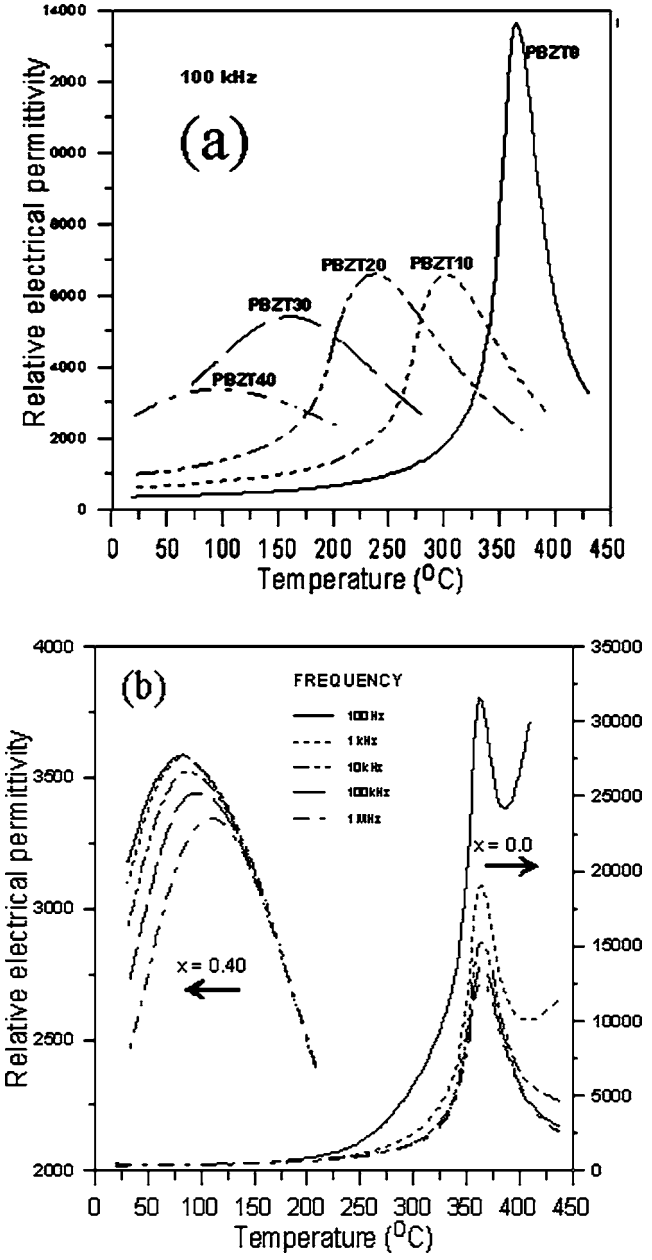

FIG. 4. Temperature dependence of the relative electrical permittivity for (a) all PBZT compositions, measured at 100 kHz and (b) $x=0$ and $x=0.40$, at different frequencies.

of the normal-relaxor transition lies in the comprehension of the evolution of ferroelectric-ferroelastic twin patterns via changes in the interatomic interactions. A possible explanation is presented as follows.

One of the remarkable features observed in this work is that the structural spontaneous strain gradually tends to vanish with increasing the Ba^{2+} content, which reduces considerably the elastic and electric energies.[47] In addition, it has been shown that with increasing the ion-doping content a transformation from ferroelectric microsized polydomain structure into nanometer single domains is verified, which occurs simultaneously with the induction of the relaxor state.[32,45,48] Therefore, in view of the hybrid ferroic character of ordinary ferroelectrics, it is proposed that the induction of the dielectric relaxor feature in ordinary ferroelectrics via doping is always preceded by a martensitic-like-phase transition (ferroelastic-paraelastic). However, in contrast to the classical first-order structural transformations, it is verified that the normal-relaxor crossover does not present an abrupt change from the product (rhombohedral, for our case) to the parent (cubic in average) phase. Rather, our present data, and the previous one obtained from $Pb_{1-x}La_xTiO_3$ ceramics,[40] reveal that local lattice distortions around Ti^{4+} atoms still persists even for high amount of doping, which shows clearly that the parent phase is not totally reached. These distortions may be related to the presence of localized nanosized polar regions (nanodomains). Therefore, we must consider some additional effects in this particular martensitic transformation to explain the formation and stabilization of these no-cubic local phases and consequent appearances of the dielectric relaxor behavior.

Let us analyze the normal-relaxor crossover in view of martensitic transformations, however, taking into account the relaxor ferroelectric peculiarities. It is well known that multiple microsized patterns of elastic domains (twins) are formed during the paraelectric-ferroelectric phase transition as a mechanism of reducing elastic strain energy,[23,49] which are stabilized by long-range elastic interactions.[20,24,50] Nevertheless, our data suggest that the continuous addition of isovalent ions changes the interaction parameters and lengths of different bonds (interatomic interactions) producing asymmetric lattice distortions, thus producing considerable changes in the unit-cell volume and the lattice parameters.[51,52] Then, for high concentrations of doping, their disordering effect tends to both destabilize the ordered phase (product or rhombohedral) and shift the thermodynamic equilibrium towards the disordered phase (parent or cubic). Thus, the elastic strain energy is significantly reduced and the domain pattern passes from a microsized polydomain structure to a single-domain structure. In this situation, although the dielectric permittivity peak becomes diffuse, it still does not present the dielectric relaxation process. Finally, on further sufficient increase of the amount of isovalent ions, the single-domain structure tends to transform into a nonpolar (no-strained or cubic) matrix, in which the elastic energy is drastically reduced. This stage corresponds to the appearance of the dielectric relaxation, the signature of relaxor ferroelectrics. In this case, however, several kinds of constraints (inhomogeneities) such as interfaces, surface effects, and lattice defects (vacancies) inherent to the processing[53,54] becomes dominant. In the case of isovalent ion substitution, the different ionic radii and electronegativities should be also considered. Indeed, we suppose that these constraints are directly responsible for the formation and stabilization of the pretransitional phase, which means the no-cubic local phases (nanodomains), between the product and parent phases. Therefore, it is proposed that lattice defects as well as surface and/or interface effects act as "seeds" to form and stabilize nanometric-polar-tweed structures with local electrical polarization (nanodomains), which are in turn embedded in a non-polar or no-strained matrix, in the ferroelectric-relaxor crossover. Consequently, the presence of such polar-tweed textures, with weak-coupled electrical interaction and a wide spectrum of relaxation times, would be

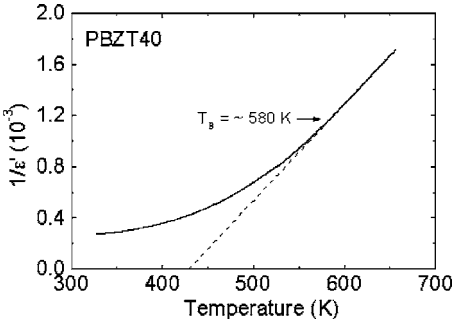

FIG. 5. Plot of $1/\varepsilon'$ vs T for the PBZT40 ceramic.

responsible for the well-known dielectric relaxor behavior. Similar concepts, also based on the conventional martensitic transformation, have been adopted to explain the origin of adaptive ferroelectric states, however, near a morphotropic phase boundary between two ferroelectric phases.[24,55] Our concepts are also consistent with the grain-size-induced relaxor crossover.[35–37]

Finally, it is also believed that these defect-induced polar-tweed structures are thermally stable at temperatures much higher than the temperature of the maximum of the dielectric permittivity (T_m). Figure 5 shows the plot of $1/\varepsilon'$ vs T for the PBZT40 ceramic ($x=0.40$). The results show that the PBZT40 present a discernible deviation from the Curie-Weiss law at $\approx$580 K, which is much higher than T_m. It has been reported that polar nanoregions persists up to the Burns temperature (T_B), where a deviation from the Curie-Weiss law is noticed.[56,57] Therefore, these results corroborate the concept that although there is no measurable remanent polarization at high temperatures ($\langle P_r \rangle = 0$), the dielectric relaxation can be related with the condensation of polar nanodomains at T_B.

It must be stressed that a pretransitional state, with glass-like behavior, stabilized by defects in conventional martensite materials (NiAl, Fe-Pd, etc.) has been commonly found in martensitic transformations.[29,50,58–60] Rather, theoretical and experimental results in martensitic transformations have shown that compositional disorder changes the microstructure from a thick twin structure to a thin one and finally to a tweed structure.[29,61] For higher concentrations of inhomogeneities, the tweed structures disappear and a disordered structure with short-range order is formed.[62,63] Moreover, it has been observed a remarkable similarity between the sequence of domain pattern states in ferroelectric and ferroic materials with increasing the amount of doping.[62,64] Similarly, it is also reported that pretransitional states in conventional martensitic transformations are stable several hundreds of degrees above the expected transition temperature.[50] Thus, all these results corroborate our assumptions.

IV. CONCLUSION

In summary, a new framework for explaining the induction of the relaxor state in ordinary ferroelectrics induced by isovalent-ion substitution is proposed. Based on the martensitic transformation ideas, it is proposed that the addition of isovalent ions in the normal ferroelectrics decreases considerably the elastic energies, thus transforming the domain patterns from a micrometer polydomain structure (twins) to nanometer-polar-tweed structures. In addition, it was also proposed that the polar-tweed structures are formed and strongly stabilized due to the presence of defects. The electrical response of these weakly coupled polar-tweed structures results in the dielectric relaxation process.

ACKNOWLEDGMENTS

The authors thank J. Mello for the sample preparation and the Brazilian agencies FAPESP and CNPq for financial support. Research was partially carried out at LNLS—National Laboratory of Synchrotron Light, Brazil.

*Electronic mail: mlente@df.ufscar.br

[1] G. Smolenski and A. Agranovska, Fiz. Tverd. Tela (Leningrad) **1**, 1562 (1960) [Sov. Phys. Solid State **1**, 1429 (1960)].
[2] P. Bonneau, P. Garnier, G. Calvarin, E. Husson, J. R. Gavarri, A. W. Hewat, and A. Morell, J. Solid State Chem. **91**, 350 (1991).
[3] Z. G. Ye, Y. Bing, J. Gao, A. A. Bokov, P. Stephens, B. Noheda, and G. Shirane, Phys. Rev. B **67**, 104104 (2003).
[4] X. H. Dai, Z. Xu, and D. Viehland, Philos. Mag. B **70**, 33 (1994).
[5] V. V. Laguta, M. D. Glinchuk, S. N. Nokhrin, I. P. Bykov, R. Blinc, A. Gregorovic, and B. Zalar, Phys. Rev. B **67**, 104106 (2003).
[6] G. Burns and F. H. Dacol, Solid State Commun. **13**, 423 (1973).
[7] L. E. Cross, Ferroelectrics **76**, 241 (1987).
[8] D. Viehland, S. J. Jang, L. E. Cross, and M. Wuttig, J. Appl. Phys. **68**, 2916 (1990).
[9] V. Westphal, W. Kleemann, and M. D. Glinchuk, Phys. Rev. Lett. **68**, 847 (1992).
[10] R. Pirc and R. Blinc, Phys. Rev. B **60**, 13470 (1999).
[11] N. Setter and L. E. Cross, J. Appl. Phys. **51**, 4356 (1980).
[12] P. M. Gehring, S. Wakimoto, Z. G. Ye, and G. Shirane, Phys. Rev. Lett. **87**, 277601 (2001).
[13] S. Miao, J. Zhu, X. Zhang, and Z. Y. Cheng, Phys. Rev. B **65**, 052101 (2001).
[14] B. Noheda, D. E. Cox, G. Shirane, J. Gao, and Z.-G. Ye, Phys. Rev. B **66**, 054104 (2002).
[15] Z.-G. Ye, Y. Bing, J. Gao, A. A. Bokov, P. Stephens, B. Noheda, and G. Shirane, Phys. Rev. B **67**, 104104 (2003).
[16] M. H. Lente, A. L. Zanin, S. B. Assis, I. A. Santos, J. A. Eiras, and D. Garcia, J. Eur. Ceram. Soc. **24**, 1529 (2004).
[17] K. Aizu, Phys. Rev. B **2**, 754 (1970).
[18] R. E. Newnham and S. Trolier-McKinstry, Integr. Ferroelectr. **20**, 1 (1998).
[19] N. A. Pertsev and A. Yu. Emelyanov, Phys. Rev. B **65**, 174115 (2002).

[20] S. Nambu and D. A. Sagala, Phys. Rev. B **50**, 5838 (1994).
[21] E. Fatuzzo and W. J. Merz, *Ferroelectricity* (Wiley, New York, 1967).
[22] Franco Jona and G. Shirane, *Ferroelectric Crystals*, 1st ed. (Pergamon, New York, 1962), Vol. 1, Chap. 3, p. 227.
[23] W. Cao and L. E. Cross, Phys. Rev. B **44**, 5 (1991).
[24] Y. M. Jin, Y. U. Wang, A. G. Khachaturyan, J. F. Li, and D. Viehland, J. Appl. Phys. **94**, 3629 (2003).
[25] G. R. Barsch and J. A. Krumhansl, Phys. Rev. Lett. **53**, 1069 (1984).
[26] B. Horovitz, G. R. Barsch, and J. A. Krumhansl, Phys. Rev. B **43**, 1021 (1991).
[27] B. Zalar, V. V. Laguta, and R. Blinc, Phys. Rev. Lett. **90**, 037601 (2003).
[28] T. Miyanaga, D. Diop, S. I. Ikeda, and H. Kon, Ferroelectrics **274**, 41 (2002).
[29] S. R. Shenoy, T. Lookman, A. Saxena, and A. R. Bishop, Phys. Rev. B **60**, R12537 (1999).
[30] Y. L. Li, S. Y. Hu, Z. K. Liu, and L. Q. Chen, Appl. Phys. Lett. **78**, 3878 (2001).
[31] X. Dai, Z. Xu, and D. Viehland, J. Appl. Phys. **79**, 1021 (1996).
[32] S. M. Gupta, J. F. Li, and D. Viehland, J. Am. Ceram. Soc. **81**, 557 (1998).
[33] G. A. Samara, J. Appl. Phys. **84**, 2538 (1998).
[34] B. G. Kim, S. M. Cho, T. Y. Kim, and H. M. Jang, Phys. Rev. Lett. **86**, 3404 (2001).
[35] Y. Park, W. J. Lee, and H. G. Kim, J. Phys.: Condens. Matter **43**, 9445 (1997).
[36] C. Ziebert, H. Schmitt, J. K. Krüger, A. Sternberg, and K. H. Ehses, Phys. Rev. B **69**, 214106 (2004).
[37] M. T. Buscaglia, V. Buscaglia, M. Viviani, J. Petzelt, M. Savinov, L. Mitoseriu, A. Testino, P. Nanni, C. Harnagea, Z. Zhao, and M. Nygren, Nanotechnology **15**, 1113 (2004).
[38] H. M. Rietveld, J. Appl. Crystallogr. **2**, 65 (1969).
[39] A. C. Larson and R. B. Von Dreele, *GSAS—Generalized Structure Analysis System* (Los Alamos National Laboratory, 1996).
[40] P. P. Neves, A. C. Doriguetto, V. R. Mastelaro, L. P. Lopes, Y. P. Mascarenhas, A. Michalowicz, and J. A. Eiras, J. Phys. Chem. Solids **108**, 14840 (2004).
[41] T. Y. Kim, H. M. Jang, and S. M. Cho, J. Appl. Phys. **91**, 336 (2002).
[42] T. Y. Kim and H. M. Jang, Appl. Phys. Lett. **77**, 3824 (2000).
[43] J. Handerek, Z. Ujma, C. Carabatos-Nédelec, G. E. Kugel, D. Dmytrow, and I. El-Harrad, J. Appl. Phys. **73**, 367 (1993).
[44] B. P. Pokharel and D. Pandey, J. Appl. Phys. **88**, 5364 (2000).
[45] Z. Xu, X. Dai, J. F. Li, and D. Viehland, Appl. Phys. Lett. **68**, 1628 (1996).
[46] B. Noheda, D. E. Cox, G. Shirane, J. A. Gonzalo, L. E. Cross, and S. E. Park, Appl. Phys. Lett. **74**, 2059 (1999).
[47] E. K. Akdogan, C. J. Rawn, W. D. Porter, E. A. Payzant, and A. Safari, J. Appl. Phys. **97**, 084305 (2005).
[48] X. Zhu, J. Zhu, S. Zhou, Q. Li, Z. Meng, Z. Liu, and N. Ming, J. Eur. Ceram. Soc. **20**, 1251 (2000).
[49] G. Arlt, J. Mater. Sci. **25**, 2655 (1990).
[50] S. Kartha, J. A. Krumhansli, J. P. Sethna, and L. K. Wickham, Phys. Rev. B **52**, 803 (1995).
[51] S. Tsunekawa, K. Ishikawa, Z. Q. Li, Y. Kawazoe, and A. Kasuya, Phys. Rev. Lett. **85**, 3440 (2000).
[52] S. Tsunekawa, S. Ito, T. Mori, K. Ishikawa, Z. Q. Li, and Y. Kawazoe, Phys. Rev. B **62**, 3065 (2000).
[53] R. E. Cohen, J. Phys. Chem. Solids **61**, 139 (2000).
[54] C. A. Randall, N. Kim, J. P. Kucera, W. Cao, and T. R. Shrout, J. Am. Ceram. Soc. **81**, 677 (1998).
[55] D. Viehland, J. Appl. Phys. **88**, 4794 (2000).
[56] G. Burns and F. H. Dacol, Solid State Commun. **48**, 853 (1983).
[57] D. Viehland, S. J. Jang, L. E. Cross, and M. Wuttig, Phys. Rev. B **46**, 8003 (1992).
[58] I. M. Robertson and C. M. Wayman, Philos. Mag. A **48**, 421 (1983); **48**, 443 (1983); **48**, 629 (1983).
[59] H. Seto, Y. Noda, and Y. Yamada, J. Phys. Soc. Jpn. **59**, 965 (1990).
[60] X. Ren and K. Otsuka, MRS Bull. **27**, 115 (2002).
[61] S. Kartha, T. Castán, J. A. Krumhansl, and J. P. Sethna, Phys. Rev. Lett. **67**, 3630 (1991).
[62] S. Semenovskaya, Y. Zhu, M. Suenaga, and A. G. Khachaturyan, Phys. Rev. B **47**, 12182 (1993).
[63] Z.-X. Cai, Y. Zhu, and D. O. Welch, Phys. Rev. B **46**, 11014 (1992).
[64] D. Viehland, M.-C. Kim, Z. Xu, and J.-F. Li, Appl. Phys. Lett. **67**, 2471 (1995).